Electronic Supplementary Material (ESI) for New Journal of Chemistry.

Supporting Information

Self-assembled organic molecules with fused aromatic ring as hole-transport layers for inverted perovskite solar cells: the effect of linker on performance

Haoliang Cheng[a,] * *and Zu-Sheng Huang*[b] *

[a] *School of Materials Science and Engineering, NingboTech University, No. 1 South Qianhu Road, Ningbo, P. R. China*

[b] *School of Pharmaceutical Sciences, Wenzhou Medical University, Wenzhou, 325035, PR China*

*Corresponding author, E-mail address: haoliang.cheng@nbt.edu.cn; huangzusheng@wmu.edu.cn

Experimental Section

Materials: *N,N*-dimethylformamide (DMF, 99.8%), dimethyl sulfoxide (DMSO, 99.8%), and chlorobenzene (CB, 99.5%) were purchased from Sigma–Aldrich. PTAA and Methylammonium iodide (MAI, 99.5%) were purchased from Xi'An Polymer Light Technology Corp. Lead iodide (PbI_2, 99.9985%) was purchased from Alfa Aesar. [6,6]-Phenyl C61 butyric acid methyl ester (PCBM, 99%) was purchased from American Dye Source, Inc. 2,9-Dimethyl-4,7-diphenyl-1,10-phenanthroline (BCP) was purchased from J&K Scientific Reagent Co. Ltd. All reagents were used as received without further purification.

The two SAMs FNE29[1] and DT-1[2] are synthesized according to the previous work. The NMR data is measured and listed below:

FNE29: ^{1}H NMR (400 MHz, CD_2Cl_2, δ): 8.32 (s, 1H), 7.29–7.31 (m, 2H), 7.17 (t, J = 7.2 Hz, 4H), 6.81–7.01 (m, 11H), 2.63–2.70 (m, 6H), 1.47–1.54 (m, 6H), 1.10–1.30 (m, 18H), 0.73–0.78 (m, 9H).

DT-1: ^{1}H NMR (400 MHz, THF-d_8) δ 8.42 (s, 1H), 8.12 (s, 1H), 7.67–7.65 (m, 2H), 7.60 (s, 1H), 7.29–7.25 (m, 4H), 7.13–7.09 (m, 6H), 7.05–7.01 (m, 2H), 4.79 (t, J = 7.0 Hz, 2H), 4.61 (m, 4H), 2.20–2.13 (m, 2H), 1.85–1.78 (m, 4H), 1.45–1.32 (m, 6H), 1.16–1.12 (m, 12H), 0.92–0.89 (m, 3H), 0.77–0.73 (m, 6H).

Device Fabrication: The In doped tin oxide (ITO, 10 Ω per square, transmittance 88%, Shenzhen Huayu United Technology Co., Ltd) glass substrates were cleaned by a sonication of 30 min in detergent, deionized water, acetone and isopropyl alcohol before being dried with a nitrogen flow. The cleaned substrates were then treated with plasma for 15 min. The ITO substrates were immersed into the SAMs solutions (0.2 mM FNE29 or DT-1 in CH_2Cl_2) for 3 h. The ITO substrates were then withdrawn from the SAM solutions and washed with CH_2Cl_2 to remove the physically absorbed molecules followed by drying with a nitrogen flow. As for the deposition of perovskite layer, the

perovskite precursor solution containing MAI (1.20 M) and PbI_2 (1.26 M) in a mixture solvent of DMF and DMSO (volume ratio of 4:1) was spin-coated on the ITO substrates without or with self-assembled dye molecules at 5000 rpm for 33 s, and the anti-solvent (CB, 300 μL) was quickly dropped onto the center of the substrate at the 13th second. Then these films were heated at 60 ^{o}C for 30 s and 100 ^{o}C for 5 min, respectively. After the above samples were cooled down to room temperature, the PCBM (20 mg cm^{-3}) solution was spun over the above films at 1600 rpm for 30 s. Then the BCP (0.5 mg/mL in isopropanol) solution was spun at 3000 rpm for 30 s. Finally, the films were transferred to a vacuum chamber, and 100 nm thick Ag electrode was deposited on top of the BCP layer with a deposition rate of 1 Å s^{-1}. The device area was defined as 0.21 cm^2. A mask with an aperture area of 0.09 cm^2 is used for all measurements of solar cell performance. For the PTAA based HTL, the PTAA solution (2 mg/mL) is spin-coated on ITO substrate at 5000 rpm for 30 s and heated at 100 ^{o}C for 10 min.

Characterization: UV-Vis absorption spectra were recorded on a UV-Vis spectrophotometer (Shimadzu UV-2550). Photoluminescence (PL) spectra were measured using a spectrofluorophotometer (RF-5301PC, Shimadzu). Differential pulsed voltammetry (DPV) were performed on an electrochemistry workstation (CHI660C Instruments, Shanghai Chenhua Instrument Corp., Shanghai, China). An $Ag/AgNO_3$ electrode, an ITO/dye electrode and a Pt electrode were used as the reference electrode, working electrode and counter electrode, respectively, using 0.1 M $TBAPF_6$ in CH_3CN as the supporting electrolyte. The electrochemical impedance spectroscopy (EIS) measurement was carried out on an electrochemical workstation (ZAHNER ZENNIUM CIMPS-1, Germany). NMR spectra were measured on Bruker 400 instruments. Contact angles were measured on Dataphysics-OCA20. Film morphology was examined with a field emission scanning electron microscope (FE-SEM-4800-1). Current density–voltage (*J–V*) characteristics of the solar cells were measured at AM1.5G illumination (100 mW cm^{-2}) with a computer-controlled Keithley 2420 source

meter and Newport-94043A solar simulator. The active area of each cell was 0.09 cm^2 controlled by a black mask. The steady-state efficiency and photocurrent outputs versus time were measured by applying a bias potential at the maximum power output point. The incident photon-to-electron conversion efficiency (IPCE) spectra were recorded on a SM-250 hyper mono-light system (Bunkoukeiki, Japan). The differential scanning calorimetry (DSC) is measured through thermal analyzer (SDT650).

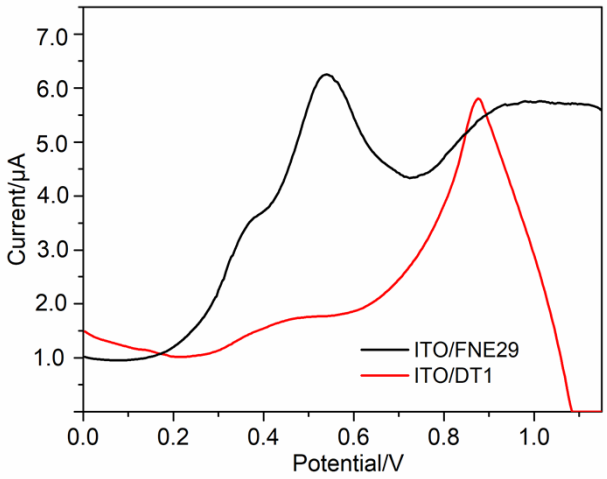

Figure S1. DPV curves of ITO/FNE29 and ITO/DT-1. The energy is converted to the vacuum scale according to the formula of $E_{HOMO} = -(E_{ox} + 4.50)$ (eV).

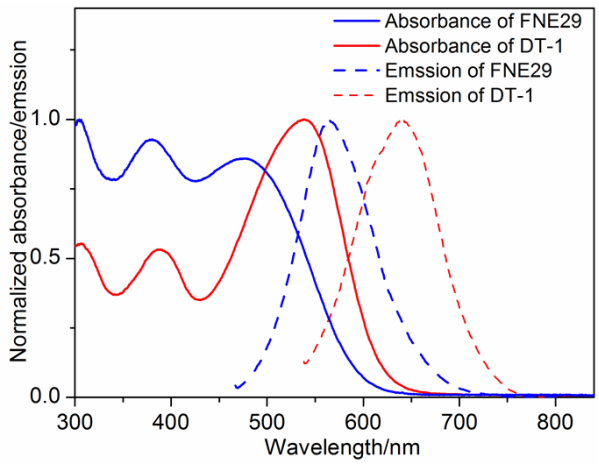

Figure S2. Normalized absorption and emssion spectra of FNE29 and DT-1 solutions in CH_2Cl_2.

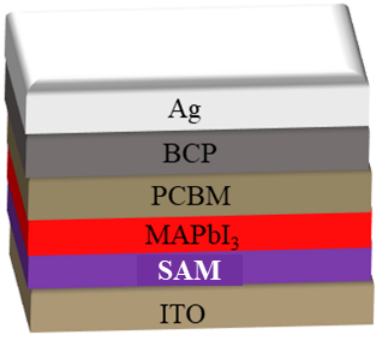

Figure S3. The PSC device configuration.

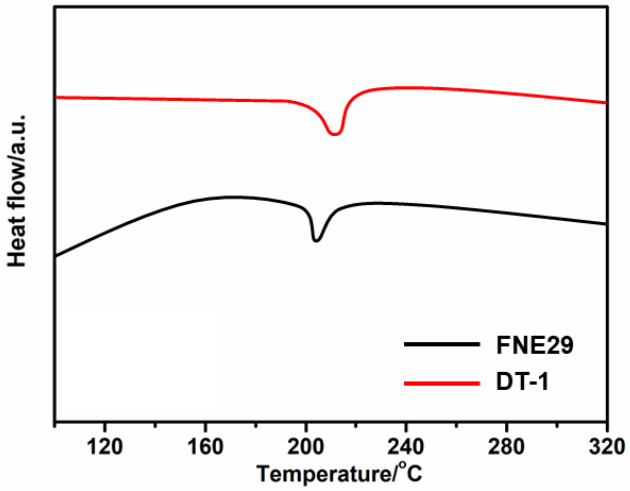

Figure S4. Differential scanning calorimetry curves of FNE29 and DT-1.

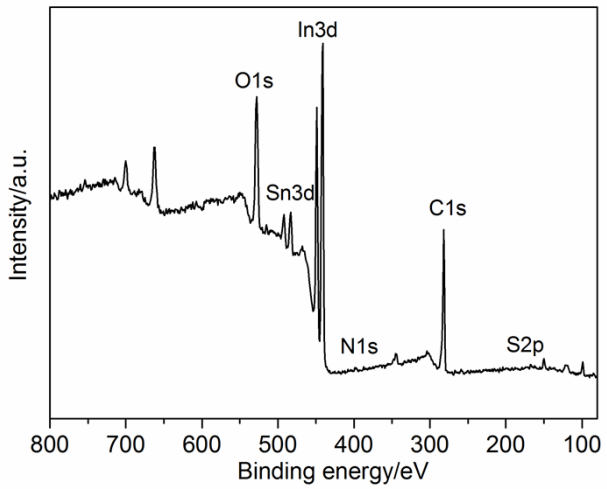

Figure S5. The XPS survey spectrum of ITO/FNE29.

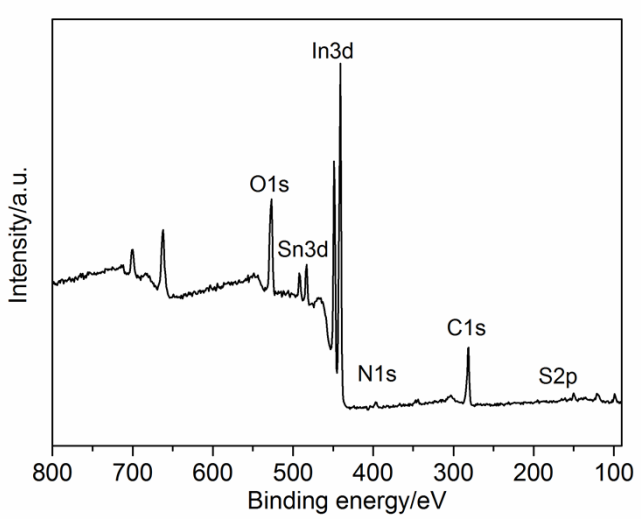

Figure S6. The XPS survey spectrum of ITO/DT-1.

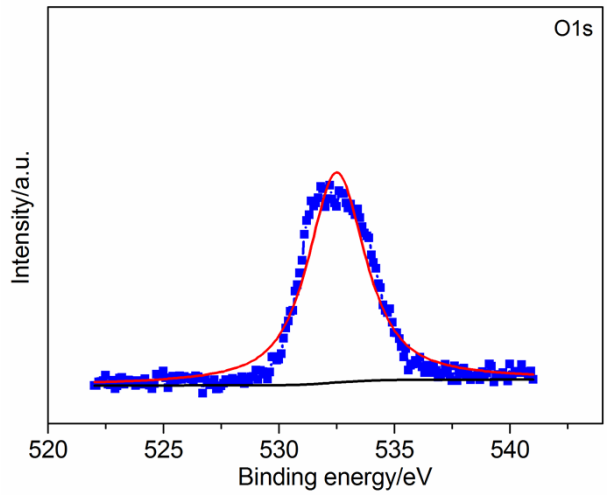

Figure S7. The high-resolution O1s XPS spectrum of the DT-1 powder.

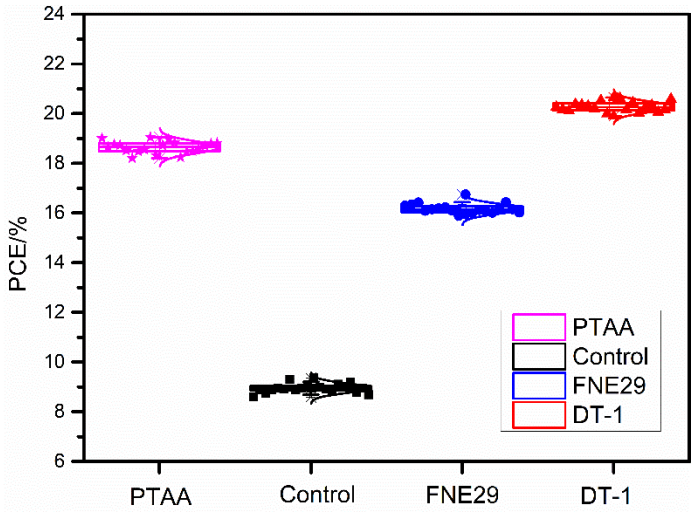

Figure S8. The statistic results of PCEs represented in a standard box plot for 20 parallel PSC devices.

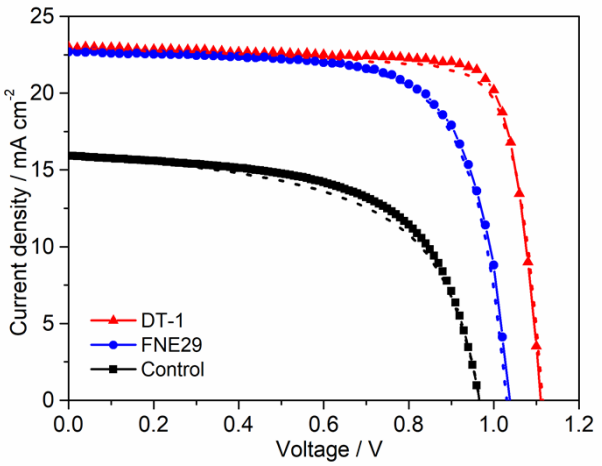

Figure S9. *J-V* curves of the SAMs based PSC with forward and reverse scan directions.

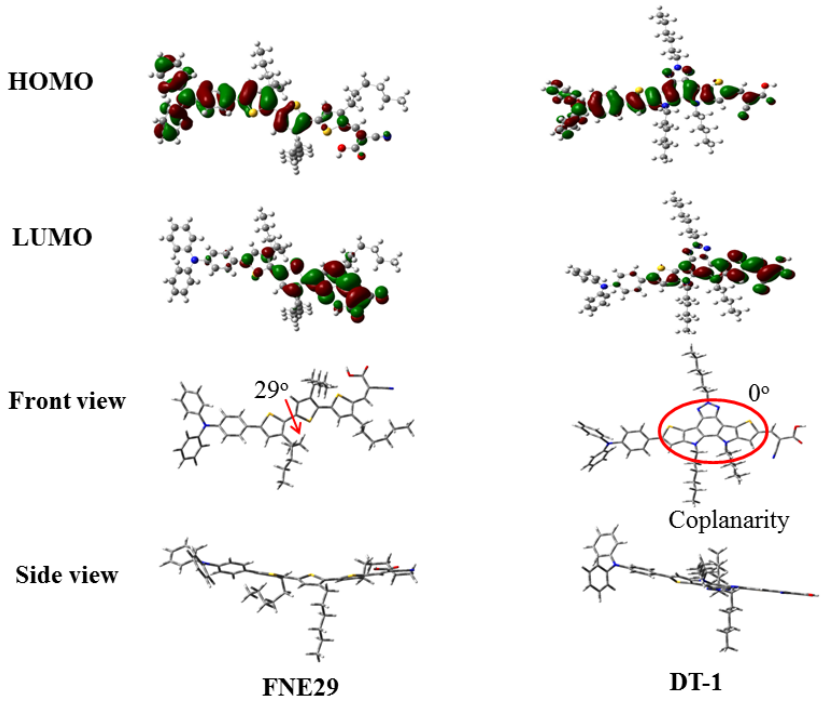

Figure S10. Electron distributions and geometrical configurations of FNE29 and DT-1.

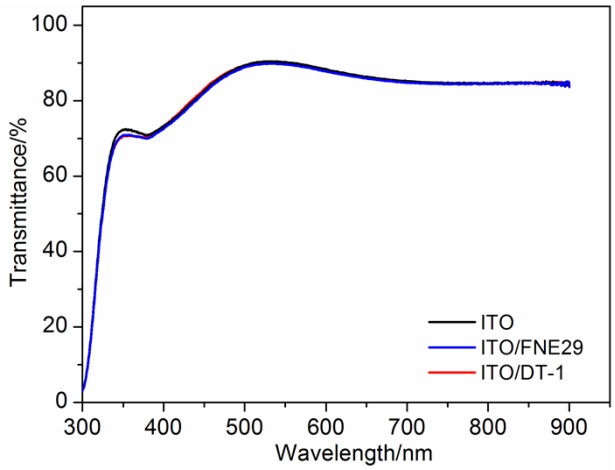

Figure S11. Transmittance of the ITO with and without SAMs.

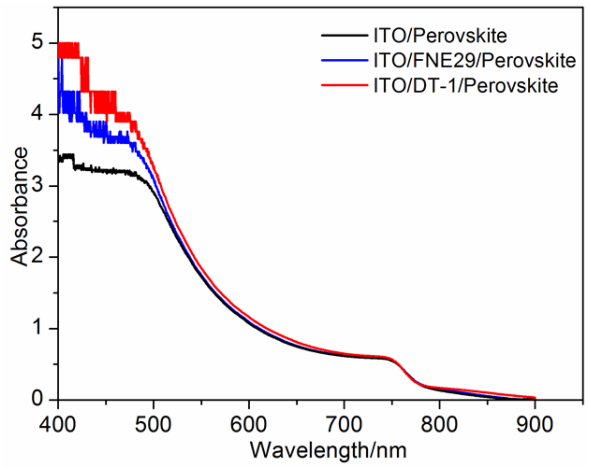

Figure S12. UV-vis absorption spectra of the perovskite films without and with SAMs.

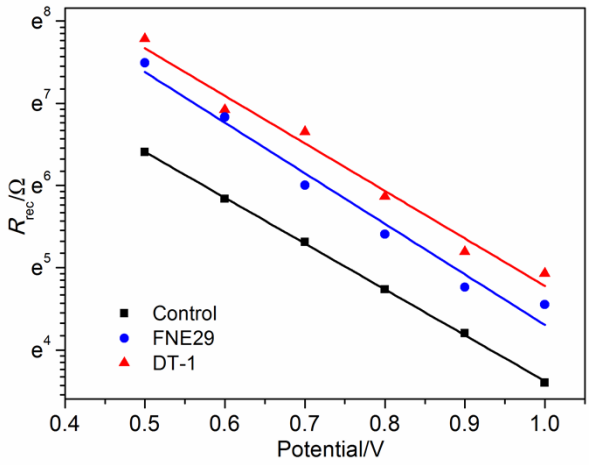

Figure S13. The charge recombination resistances (R_{rec}) *vs*. potential for various PSCs.

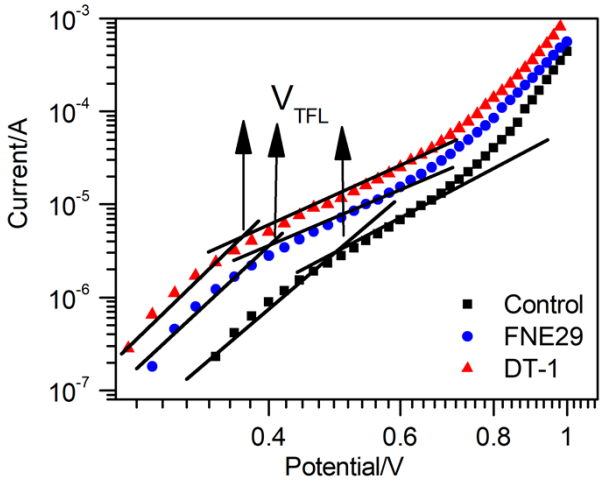

Figure S14. The dark current curve of the hole only device with a structure of ITO/SAMs/Perovskite/Spiro-OMeTAD/Au.

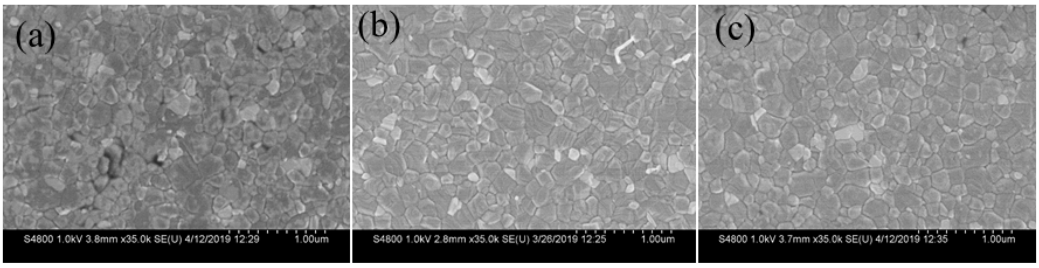

Figure S15. The SEM images of perovskite films on (a) ITO, (b) ITO/FNE29, and (c) ITO/DT-1, respectively.

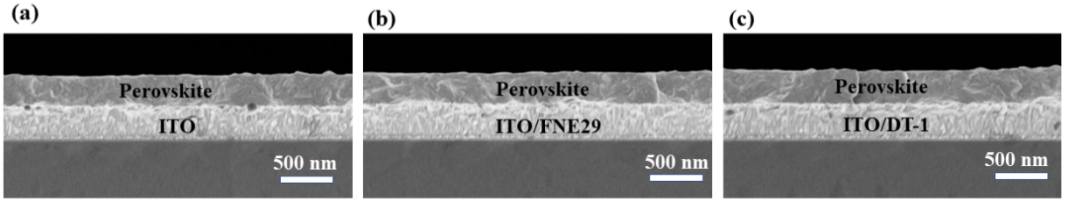

Figure S16. The Cross-sectional SEM images of perovskite films on (a) ITO, (b) ITO/FNE29, and (c) ITO/DT-1, respectively.

Table S1. Optical, electrochemical and hole mobility data of FNE29 and DT-1.

	λ_{max} (nm)[a]	λ_{int} (nm)[b]	$E_{0\text{-}0}$ (eV)[c]	HOMO (eV)[d]	LUMO (eV)[f]	Hole mobility ($cm^2\ V^{-1}\ s^{-1}$)[e]
FNE29	478	532	2.33	-5.04	-2.71	2.31×10^{-4}
DT-1	538	584	2.12	-5.37	-3.25	4.34×10^{-4}

[a] Absorption maximum measured in CH_2Cl_2 with concentration of 1×10^{-5} mol dm^{-3}; [b] intersection wavelength obtained from the cross point of normalized absorption and emission spectra in CH_2Cl_2 solution; [c] $E_{0-0} = 1240/\lambda_{int}$; [d] the HOMO data obtained from the DPV measurements; the energy is converted to the vacuum scale according to the formula of $E_{HOMO} = -(E_{ox} + 4.50)$ (eV); [e] the hole mobility of the SAMs measured with a device structure of ITO/PEDOT:PSS/SAMs/Ag; [f] the LUMO is calculated according to the formula of $E_{LUMO} = (E_{0-0} + E_{HOMO})$ (eV)

Table S2. Photovoltaic performance parameters of each best-performing PSC device. Measurements were performed under different scan directions.

Device	Scan directions	V_{oc} (V)	J_{sc} (mA cm^{-2})	*FF*	*PCE* (%)	*HI (%)*
Control	Forward	0.966	15.91	0.609	9.36	5.76
	Reverse	0.968	16.08	0.568	8.85	

ITO/FNE29	Forward	1.038	22.68	0.712	16.75	1.89
	Reverse	1.030	22.65	0.705	16.44	
ITO/DT-1	Forward	1.110	23.00	0.809	20.65	2.58
	Reverse	1.115	22.94	0.787	20.13	
ITO/PTAA	Forward	1.092	22.75	0.767	19.05	2.99
	Reverse	1.089	22.56	0.752	18.48	

$HI = (PCE_{Forward} - PCE_{Reverse})/PCE_{reverse}$

Table S3. The EIS fitting parameters of the as-prepared devices, measured at bias potential of 1 V under dark.

PSC	R_s (Ω)	R_{rec} (Ω)
Control	14.4	36.5
FNE29	26.8	94.5
DT-1	17.5	138.2

References

1. Feng, Q.; Zhou, G.; Wang, Z.-S., Varied Alkyl Chain Functionalized Organic Dyes for Efficient Dye-Sensitized Solar Cells: Influence of Alkyl Substituent Type on Photovoltaic Properties. *J. Power Sources* **2013**, *239*, 16-23.

2. Huang, Z.-S.; Hua, T.; Tian, J.; Wang, L.; Meier, H.; Cao, D., Dithienopyrrolobenzotriazole-Based Organic Dyes with High Molar Extinction Coefficient for Efficient Dye-Sensitized Solar Cells. *Dyes Pigm.* **2016**, *125*, 229-240.